Optimization of Leaf Nutrient Mapping in Oil Palm A Geospatial Comparison for Site-Specific Management

Wiratmoko, D.,[1,4] Sabrina, T.,[2*] Minasny, B.[3] and Nasution, Z.[2]
[1]Agricultural Science Doctoral Program, Faculty of Agriculture, Universitas Sumatera Utara (USU), Jl. Dr. A. Sofian No.3, Sumatera Utara, Indonesia, E-mail: dhimas.wiratmoko@students.usu.ac.id
[2]Faculty of Agriculture, Universitas Sumatera Utara (USU), Jl. Dr. A. Sofian No.3, Sumatera Utara, Indonesia, E-mail: t.sabrina@usu.ac.id,* zulnasution@usu.ac.id
[3]Sydney Institute of Agriculture, C81–Biomedical Building, The University of Sydney, Australia E-mail: budiman.minasny@sydney.edu.au
[4]Indonesian Oil Palm Research Institute, Jl. Brigjen Katamso No. 51, Medan, Sumatera Utara, Indonesia, E-mail: dhimaswiratmoko@iopri.org
Corresponding Author

DOI: https://doi.org/10.52939/ijg.v21i9.4447

Abstract
Accurate nutrient mapping is crucial to optimize fertilizer application and ensure sustainable oil palm production. In this study, four spatial interpolation methods, including Inverse Distance Weighting (IDW), Ordinary Kriging (OK), Universal Kriging (UK), and Radial Basis Function (RBF), were evaluated and compared to estimate leaf macronutrient content in oil palm plantations across North Sumatra, Indonesia. A total of 3,191 georeferenced leaf samples were collected from the 17th frond and analyzed for nitrogen (N), phosphorus (P), potassium (K), calcium (Ca), and magnesium (Mg). Spatial interpolation was conducted using each method, and performance was evaluated based on the Mean Error (ME), Mean Absolute Error (MAE), Root Mean Square Error (RMSE), and Mean Absolute Percentage Error (MAPE). The results showed that all methods achieved acceptable prediction accuracy, with MAPE values ranging from 3% to 10%. OK and IDW performed optimally across most nutrients, with excellent predictions for nitrogen, potassium, calcium, and magnesium. The resulting maps facilitated site-specific nutrient management, offering a cost-effective and environmentally friendly alternative to uniform fertilization practices. This study supports precision agriculture by enabling an accurate site-specific nutrient diagnosis across extensive oil palm plantations.

Keywords: Leaf nutrient, Oil palm, Precision agriculture, Site-specific nutrient management, Spatial interpolation

1. Introduction

Oil palm (*Elaeis guineensis* Jacq.) is a plant that plays a crucial role in Indonesia's economic structure, significantly affecting employment, export revenue, and national income [1]. To increase oil palm yields and promote sustainable agricultural practices, careful nutrient management is essential. Undetected or inaccurately assessed nutrient deficiencies can lead to reduced yields and long-term degradation of soil fertility [2]. The application of fertilizers accounts for a significant portion of the production costs in oil palm cultivation, comprising 30–65% of the total field maintenance expenses [3][4] and [5]. The increasing cost of fertilizers further prompts the need for efficient nutrient management strategies [6]. Precise application is critical for cost-effectiveness and optimal plant health. Essential macronutrients such as nitrogen (N), phosphorus (P), potassium (K), calcium (Ca), and magnesium (Mg) are required in adequate amounts for healthy growth and development of oil palm plants under normal conditions [2]. Physiological roles of the key nutrients studied (N, P, K, Ca, and Mg) in oil palm growth and productivity. Nitrogen is a critical requirement for vegetative growth and leaf development, phosphorus supports root development and energy transport, potassium enhances oil synthesis and stress tolerance, calcium strengthens cell walls and root function, and magnesium is central to chlorophyll formation and photosynthesis. These nutrients directly affect the yield and plantation sustainability. Deficiencies in these nutrients can be identified based on the visible symptoms [1].

Leaf nutrient content analysis is widely used diagnostic method [7]. However, traditional nutrient diagnosis methods often rely on critical levels or sufficient ranges, which may not accurately reflect site-specific variability [7] and [8]. Factors such as genotype, soil nutrient concentration, frond sampling level, and plant age significantly influenced the interpretation of the leaf nutrient data.

Nutrient deficiencies can be assessed through soil and leaf analyses; however, nutrient diagnosis is considered an empirical method that requires standardized leaf sampling units (LSU), accurate sampling time, and laboratory testing, all of which are costly and time-consuming [8]. To enable timely and accurate fertilization planning, it is essential to use spatial tools capable of predicting nutrient content in unsampled areas. Geostatistical methods, such as Inverse Distance Weighting (IDW), Ordinary Kriging (OK), Universal Kriging (UK), and Radial Basis Function (RBF), are effective for modeling spatial variations in soil and leaf nutrient content [9]. Numerous studies have used interpolation methods to evaluate the soil properties. For example, IDW and RBF were used to estimate the total phosphorus content in China, whereas OK, co-kriging (COK), random forest (RF), and artificial neural networks (ANN) were applied for soil property mapping in alluvial plains [10] and [11]. Additional methods, such as regression kriging (RK), geographically weighted regression kriging (GWRK), and multiscale geographically weighted regression kriging (MGWRK), have been used as soil fertility indicators, including organic matter, nitrogen, phosphorus, and potassium [12]. Comparative analyses of Kriging and IDW across various areas, such as Kentucky, Ethiopia, and Korea, validated the applicability of spatial analysis for nutrient mapping [13][14] and [15]. In Malaysia, Geographic Information System (GIS)-based methods have been used to spatially represent the nutrient content of oil palm plantations [16].

Based on the described advancements, this study aimed to map the spatial distribution of leaf macronutrients in oil palm plantations using four common interpolation methods (IDW, OK, UK, and RBF) and evaluate the relative performance based on predictive accuracy. The use of a large georeferenced dataset (3191 samples) in North Sumatra enabled comprehensive spatial modeling and provided insights into site-specific nutrient management strategies.

2. Materials and Methods

2.1 Study Area

This study was conducted in an oil palm plantation area in North Sumatra Province. The study area was defined based on the 2019 oil palm land cover map issued by the Ministry of Agriculture of Indonesia through Decree No. 833/KPTS/SR.020/M/12/2019. The study area spans 2,079,027 hectares at the coordinates 97°57′16.5″ to 100°24′25.7″ and 0° 14′55.8″ to 4°17′48.2″, while the spatial distribution of the sample points is shown in Figure 1.

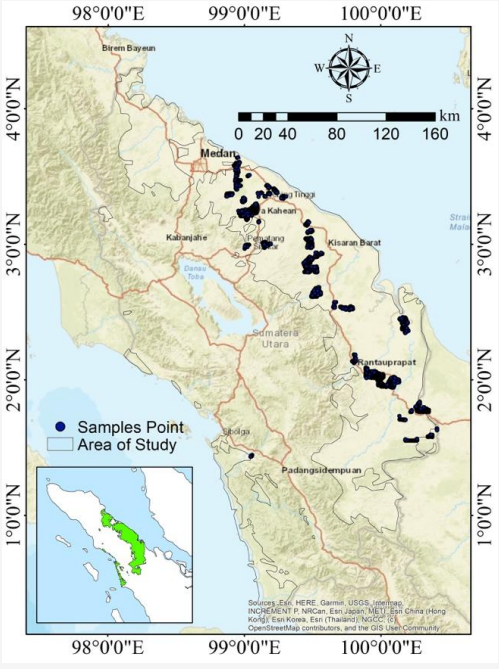

Figure 1: Map of the study area in North Sumatera

This study assumed uniformity in plant conditions, environmental factors (including climate and soil type), and management practices.

2.2 Data Source (Oil Palm Leaf Analysis Data)

This study used secondary data from laboratory analysis of macronutrient content, including nitrogen, phosphorus, potassium, calcium, and magnesium, collected from the 17th frond of oil palm leaves. A total of 3,191 georeferenced sample points from North Sumatra Province were analyzed in 2019. The collected leaf samples were sent to a certified laboratory for chemical analysis of five key macronutrients: nitrogen (N), phosphorus (P), potassium (K), calcium (Ca), and magnesium (Mg). The analysis adhered to standard protocols for leaf tissue examination, employing the Kjeldahl method for total nitrogen, Bray-II extraction coupled with spectrophotometry for available phosphorus, and Atomic Absorption Spectrophotometry (AAS) with ammonium acetate extraction for potassium, calcium, and magnesium. The leaf nutrient levels were categorized into five classes: deficiency, slight deficiency, normal, slight excess, and excess as presents in Table 1 [17].

2.3 Spatial Interpolation

OK, UK, IDW, and RBF were the methods used in this study for spatial interpolation performed with 30–45 neighboring points [18]. Approximately 70% (2,227) and 30% (964) of the samples were used for the validation and model input data, respectively. Spatial interpolation and prediction processes were conducted using ArcMap 10.8.2. Figure 2 presents the flowchart of the general study methodology.

Table 1: Classification of nutrient content of oil palm leaf [17]

Nutrient	Nutrient Content (%)				
	Deficiency	Slight Deficiency	Normal	Slight Excess	Excess
Nitrogen (N)	<2.30	2.30-2.50	2.50-2.70	2.70-2.90	>2.90
Phosphorus (P)	<0.14	0.14-0.16	0.16-0.17	0.17-0.19	>0.19
Potassium (K)	<0.60	0.60-0.80	0.80-1.00	1.00-1.20	>1.20
Calcium (Ca)	<0.55	0.55-0.60	0.60-0.65	0.65-0.70	>0.70
Magnesium (Mg)	<0.20	0.20-0.23	0.23-0.25	0.25-0.27	>0.27

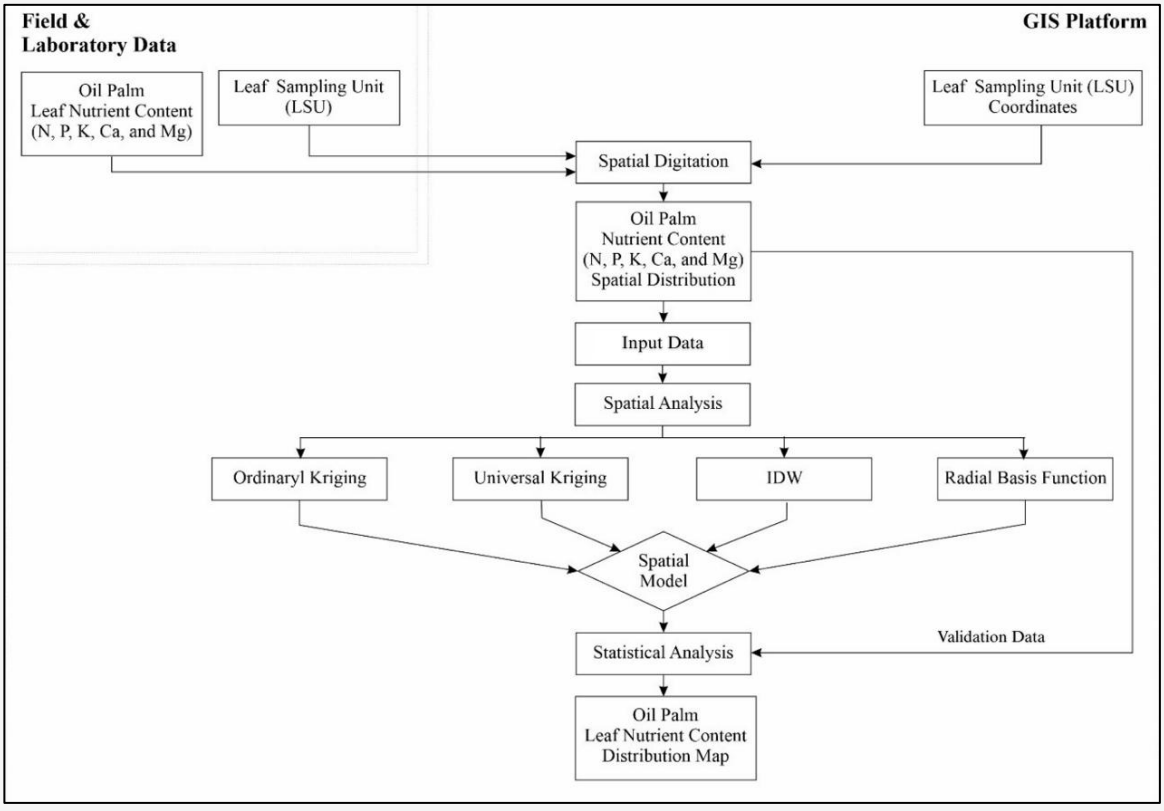

Figure 2: Oil palm leaf nutrient mapping

2.3.1 Ordinary Kriging (OK)

The OK model uses the semi-variogram theory to capture spatial autocorrelation and assumes second-order stationarity in the data distribution [9][10][11] and [12]. This method estimates unknown values based on linear unbiased predictions from the observed neighboring data points, and the estimation is defined in Equation 1:

$$\bar{Z} = \sum_{i=1}^{n} \gamma_i Z(x_i) \quad \text{Equation 1}$$

Where $\bar{Z}$ is the interpolated value, $Z(x_i)$ represents the value at the sampled area x_i, and γ_i is the weight derived from the semi-variogram.

2.3.2 Universal Kriging (UK)

The UK incorporates trends (linear or polynomial) across coordinates, allowing better modeling of nonstationary spatial processes compared to OK [18]. The UK estimation uses a trend function defined in Equations 2 and 3:

$$\bar{Z}x_0 = \sum_{i=1}^{n} \omega_i Z(x_i)$$

Equation 2

$$\bar{Z}x_0 = \beta_0 + \beta_1 \sum_{i=1}^{n} \omega_i Z(x_i)(X) + \beta_2 \sum_{i=1}^{n} \omega_i Z(x_i)(Y) + \sum_{i=1}^{n} \omega_i \delta(x_i)$$

Equation 3

Where $\bar{Z}$ is the interpolated value, $Z(x_i)$ represents the value at the sampled area xi, β_1 and β_2 are the trend coefficients, δ(xi) is the stochastic component, and ωi represents the weights.

2.3.3 Radial Basis Function (RBF)

RBF interpolation applies radial symmetric functions with polynomial terms. This method is suitable for large datasets [19] and its general form is defined in Equation 4:

$$\bar{Z} = \sum_{i=1}^{n} \lambda_i \phi\left(\left|x - x_i\right|\right) + p(x)$$

Equation 4

Where $\bar{Z}$ is the interpolated value, $Z(x_i)$ represents the value at the sampled area x_i, λ_i is the weight, φ represents the radial basis function, and $p(x)$ is the polynomial.

2.3.4 Inverse Distance Weighting (IDW)

IDW estimates unknown values as the weighted average of neighboring known values. Furthermore, closer points contribute more to the estimate [10][18] and [20], and the formula for IDW is defined in Equations 5, 6 and 7:

$$\bar{Z}(x_0) = \frac{\sum_{i=1}^{n} \bar{Z}_i d_i^{-p}}{\sum_{i=1}^{n} d_i^{-p}}$$

Equation 5

$$w_i = \frac{d_i^{-p}}{\sum_{i=1}^{n} d_j^{-p}}$$

Equation 6

$$\bar{Z}(x_0) = \omega_i \bar{Z}_i$$

Equation 7

Where $\bar{Z}(x_0)$ is the interpolated value (predicted value at the target location location x_0, $\bar{Z}_i$ represents the observed value at sample point x_i $(i=1,\ldots,n)$, and $d_i = ||x_0 - x_i||$ is the Euclidean distance between target location and sample i. $p > 0$ represented the power of parameter that controls the influence of distance. A common choice is p=2; higher values give greater weight to closer points. N is representing the number of sample point considered in interpolation and ω is represented the normalized weight assigned to sample iii, ensuring that the sum of all weights.

2.4 Statistical Analysis

In addition to the error metrics, paired t-tests were conducted to compare the predicted and actual nutrient values (N, P, K, Ca, and Mg) for each interpolation method. Paired t-tests assessed the presence of a statistically significant difference between the predicted and observed values, whereas a two-tailed test was performed at a significance level of 0.05. When the p-value exceeded 0.05, the difference was considered statistically insignificant, suggesting that the model predictions were consistent with actual measurements. This method has been widely adopted in spatial prediction validation studies [21] and [22]. Therefore, the statistical t-test complements the accuracy metrics and ensures that interpolated models are statistically valid for nutrient mapping.

2.5 Model Validation

The model accuracy for each interpolation method (OK, UK, RBF, and IDW) was evaluated using the geostatistics module of ArcMap 10.8.2. The metrics used were Mean Error (ME), Mean Absolute Error (MAE), Root Mean Square Error (RMSE), and accuracy (Acc), is defined in Equations 8, 9, 10, and 11:

$$ME = \frac{1}{n} \sum_{i=1}^{n} \left[\bar{Z}(x_i) - Z(x_i)\right]$$

Equation 8

$$MAE = \frac{1}{n} \sum_{i=1}^{n} \left[\left|\bar{Z}(x_i) - Z(x_i)\right|\right]$$

Equation 9

$$RMSE = \sqrt{\frac{1}{n} \sum_{i=1}^{n} \left[\left|\bar{Z}(x_i) - Z(x_i)\right|\right]^2}$$

Equation 10

$$Acc = \left[1 - \frac{1}{n} \sum_{i=1}^{n} \left|\frac{\bar{Z}x_i - Zx_i}{Z_i}\right|\right]$$

Equation 11

Where $\bar{Z}(x_i)$ is the predicted value, $Z(x_i)$ is the actual value, and n is the number of observations. A good model is expected to have a low ME, MAE, and RMSE, and high accuracy values [10].

3. Results

3.1 Descriptive Statistics of Spatial Analysis

A detailed descriptive statistical analysis was conducted to evaluate the spatial predictions of five key leaf nutrients, nitrogen (N), phosphorus (P), potassium (K), calcium (Ca), and magnesium (Mg), using four interpolation methods: Ordinary Kriging (OK), Universal Kriging (UK), Inverse Distance Weighting (IDW), and Radial Basis Function (RBF). The analysis aimed to assess the central tendency, distribution shape, and variability of each nutrient across different methods. While the overall means and medians were generally similar among the interpolation methods, several significant findings emerged from the variability and distribution patterns of nutrient predictions. The oil palm leaf nitrogen nutrient content presents in Table 2.

Nitrogen (N):

All four methods yielded comparable mean values for nitrogen content (2.48–2.49%) with equally consistent median values (2.49–2.50%), indicating a stable prediction of the central tendency. The small standard deviation (0.02) and modest coefficients of variation (CVs between 5.12–5.47%) across methods confirmed the low variability in N spatial distribution. However, IDW exhibited the widest range (1.92–2.97%), suggesting greater sensitivity to local extremes, whereas OK and RBF showed tighter distributions. A key observation lies in the distribution shape, where all methods demonstrated negative skewness, particularly in RBF (-1.39), indicating a tendency toward higher N values and fewer low-concentration predictions. This negatively skewed pattern could be associated with localized N accumulation under site-specific field conditions. The kurtosis values were all close to zero, indicating a mesokurtic nearly normal distribution.

Phosphorus (P):

Phosphorus showed the highest level of agreement across all statistical parameters. The mean and median values were 0.16% for all methods, indicating a very symmetrical and centered distribution**.** The modes differed slightly, ranging from 0.15 to 0.16%. The UK produced the widest range (0.12–0.19%), while the other methods yielded similar ranges. Despite having identical standard deviations (0.01), the coefficient of variation was the highest in RBF (7.31%), implying a slightly greater dispersion relative to the mean compared to OK (5.83%) or IDW (6.86%). The skewness values were close to zero (0.12–0.24), and all kurtosis values were zero, suggesting that the phosphorus predictions were symmetrical and mesokurtic, with a relatively uniform spatial distribution. These findings align with those of previous studies, indicating that leaf P content in perennial crops tends to show low spatial variability.

Potassium (K):

While the mean potassium values were similar across methods (0.90–0.91%), a sharp contrast emerged in variability and distribution. IDW and RBF exhibited very high standard deviations (0.15) compared to only 0.02–0.03 for OK and UK. Notably, IDW's CV value of IDW was implausibly low (0.78%), likely due to data recording inconsistency, while OK (16.00%), UK (17.31%), and RBF (17.03%) showed more realistic and elevated CVs. These high values indicate a substantial spatial variation in potassium content. The distribution skewness was strongly positive, especially in the UK (4.12) and OK (2.13), suggesting the prevalence of low K values with a few extreme highs. The UK also had a high kurtosis value (3.55), indicating a leptokurtic distribution with sharper peaks and heavier tails. This behavior reflects the well-known spatial heterogeneity of potassium, which is often influenced by the leaching and uptake dynamics in oil palm systems.

Calcium (Ca):

Calcium estimates were highly consistent in both the mean (0.72%) and median (0.67%) values across all methods. However, the mode varied slightly, with IDW producing the highest (0.63%) and OK/UK producing the lowest (0.61%). RBF had a broader distribution with a minimum value of 0.18%, indicating its sensitivity in capturing very low values. All methods had standard deviations of approximately 0.14, and the CVs were uniformly high (24.13–24.62%), suggesting that Ca exhibited strong spatial variability. Positive skewness values (1.22–1.24) across all methods confirmed that the calcium content was generally concentrated at the lower end, with a tail toward higher values. Low kurtosis values (0.03) indicate a distribution close to normal. These findings suggest that although Ca predictions are consistent in central values, they are more spatially variable and subject to influencing factors such as pH or cation competition.

Magnesium (Mg):

Mg content predictions were the most stable among all the nutrients. All the methods produced identical mean (0.27%) and median (0.26%) values. IDW showed the highest mode (0.27%) and CV (24.16%), whereas RBF showed the lowest mode (0.23%) and CV (19.05%), indicating that RBF predictions were more concentrated and less variable. OK and UK captured the widest range (0.08–0.52%), whereas RBF had a tighter range (0.10–0.46%). The skewness

values were modestly positive (0.47–0.68), indicating a right-skewed distribution, with higher concentrations at the lower end and some high outliers. Kurtosis remained near zero, supporting a normal-like distribution shape. This stability makes Mg a reliable nutrient for comparisons across interpolation methods.

Table 2: Descriptive analysis of oil palm leaf nitrogen nutrient content in this study

Parameter	Nutrient	OK	UK	IDW	RBF
Mean	Nitrogen	2.48	2.48	2.49	2.48
	Phosphorus	0.16	0.16	0.16	0.16
	Potassium	0.91	0.9	0.91	0.91
	Calcium	0.72	0.72	0.72	0.72
	Magnesium	0.27	0.27	0.27	0.27
Mode	Nitrogen	2.47	2.55	2.55	2.55
	Phosphorus	0.16	0.15	0.15	0.16
	Potassium	0.8	0.8	0.81	0.8
	Calcium	0.61	0.61	0.63	0.62
	Magnesium	0.25	0.25	0.27	0.23
Median	Nitrogen	2.49	2.49	2.5	2.49
	Phosphorus	0.16	0.16	0.16	0.16
	Potassium	0.89	0.87	0.9	0.89
	Calcium	0.67	0.67	0.67	0.67
	Magnesium	0.26	0.26	0.26	0.26
Min	Nitrogen	1.97	1.95	1.92	1.95
	Phosphorus	0.13	0.12	0.12	0.12
	Potassium	0.63	0.54	0.61	0.6
	Calcium	0.23	0.23	0.33	0.18
	Magnesium	0.08	0.08	0.08	0.1
Max	Nitrogen	2.82	2.84	2.97	2.84
	Phosphorus	0.18	0.19	0.18	0.19
	Potassium	1.6	1.58	1.54	1.65
	Calcium	1.22	1.21	1.33	1.21
	Magnesium	0.52	0.52	0.47	0.46
Std Dev	Nitrogen	0.02	0.02	0.02	0.02
	Phosphorus	0.01	0.01	0.01	0.01
	Potassium	0.03	0.02	0.15	0.15
	Calcium	0.14	0.14	0.14	0.14
	Magnesium	0.04	0.04	0.05	0.04
Skewness	Nitrogen	-1.17	-1.11	-0.32	-1.39
	Phosphorus	0.12	0.24	0.13	0.24
	Potassium	2.13	4.12	0.29	0.47
	Calcium	1.24	1.24	1.22	1.24
	Magnesium	0.56	0.63	0.47	0.68
Kurtosis	Nitrogen	0.02	0.02	0	0.05
	Phosphorus	0	0	0	0
	Potassium	0.25	3.55	0	0
	Calcium	0.03	0.03	0.03	0.03
	Magnesium	0	0	0	0
CV (%)	Nitrogen	5.12	5.43	5.47	5.45
	Phosphorus	5.83	7.2	6.86	7.31
	Potassium	16	17.31	0.78	17.03
	Calcium	24.25	24.13	24.62	24.57
	Magnesium	19.79	19.22	24.16	19.05

Description: Ordinary Kriging (OK), Universal Kriging (UK), Inverse Distance Weighting (IDW), (Radial Basis Function); CV (coefficient of variation)

Descriptive analysis revealed several important insights into the spatial characteristics of leaf nutrient distribution, as predicted by the four interpolations methods. First, the consistency of central tendency indicators (for example, mean, median, and mode) across all methods for nutrients, such as nitrogen, phosphorus, and magnesium, suggests that these nutrients are uniformly distributed in the study area. The low standard deviation and narrow coefficient of variation (CV) values further reinforce this interpretation. This stability implies that these nutrients are either well managed across the plantation or are less affected by spatial variability due to inherent soil or plant physiological factors.

In contrast, potassium and calcium exhibited more prominent variability, as evidenced by higher CV values (exceeding 16% for potassium and 24% for calcium), larger prediction ranges, and more pronounced skewness values. These findings indicate that these nutrients are spatially heterogeneous and may be influenced by site-specific factors, such as topography, soil texture, root distribution, or past fertilization history. The positive skewness for potassium (especially 4.12 in the UK) and calcium (1.24 across methods) suggests a prevalence of low-nutrient zones, with fewer areas exhibiting high concentrations.

The skewness and kurtosis values offer further interpretation. Nutrients, such as nitrogen, exhibit negative skewness in several methods (e.g., -1.39 RBF), suggesting a distribution biased toward higher values. This could indicate potential areas of nutrient accumulation, possibly resulting from overfertilization or inefficient nutrient uptake. In contrast, the leptokurtic distribution of potassium in the UK (kurtosis = 3.55) points to a distribution with more extreme values than a normal curve, warranting caution when interpreting spatial predictions without proper field verification.

Furthermore, the comparison between the interpolation methods highlights subtle but meaningful differences. OK and UK, grounded in geostatistical theory, generally provide smoother and more conservative predictions, whereas IDW and RBF appear to enhance the local variability by producing wider prediction ranges and higher CV values. This suggests that deterministic methods such as IDW may be more responsive to local sample clustering but are also more sensitive to data anomalies.

These findings have several practical implications. For nutrients with low spatial variability (e.g., phosphorus and magnesium), any of the four methods may yield reliable maps. However, for nutrients with high variability and asymmetry (e.g., potassium and calcium), careful selection of the interpolation method is critical to avoid misinterpretation and guide site-specific nutrient interventions. Overall, the descriptive statistics not only confirm the robustness of the interpolation outcomes, but also underscore the importance of understanding spatial data distribution in nutrient mapping. Such insights can inform targeted fertilization, support resource-efficient plantation management, and enhance the precision of agronomic decisions.

3.2 T-Test between Actual Data and Predictions from the Four Interpolation Methods for Nutrient Content (N, P, K, Ca, and Mg)

The t-test results in Table 3 showed no statistically significant differences between the actual and predicted values of nitrogen content for all interpolation methods. The p-values for all methods were far above the significance threshold of 0.05, with the highest being found in RBF ($p = 0.970$) and the lowest in IDW ($p = 0.736$), suggesting that all methods had good predictive performance for nitrogen content without introducing substantial systematic bias compared with the actual values. Similar to nitrogen, the t-test results for phosphorus content showed no significant differences between actual and predicted means. All p values were greater than 0.84, indicating a high level of prediction accuracy. OK showed slightly higher predicted values than the actual values (mean prediction = 0.915182), but the difference was not statistically significant ($p = 0.843$). This observation implies that spatial interpolation, particularly kriging, can be used to accurately model phosphorus distribution.

The analysis results for potassium showed an identical pattern to those for phosphorus because both were based on the same actual and predicted values. Although the predicted values varied slightly across the methods, none of the t-tests identified any significant differences. The p-values for the four methods ranged from 0.843–0.972, confirming that the applied interpolation methods represented the potassium distribution with a high degree of confidence. Potassium, which is highly dynamic in the soil and plants, can be accurately mapped using geospatial methods. The actual and predicted mean values for calcium were very close, and the t-test results showed that all interpolation methods produced insignificantly different predictions. The p-values ranged from 0.580 (OK) to 0.935 (IDW), suggesting that even though spatial variation in calcium is influenced by many environmental and management factors, interpolation methods, such as the UK and OK, can still provide reliable estimates. The t-test results for Mg content showed a similar pattern, as all interpolation methods produced p-

values greater than 0.5, suggesting no significant differences between the actual and predicted values. IDW produced predictions closest to the actual values (p = 0.935), followed by the RBF method (p = 0.734). In general, the t-test results for all nutrient elements showed no significant differences between the actual values and those predicted by the four interpolation methods, implying that the spatial method used could accurately represent the leaf nutrient content of the oil palm. This statistical validation strengthens the use of geospatial methods as supporting tools for decision-making in precision fertilization management, specifically in oil palm plantations.

3.3 Comparison of the Distribution of Interpolation Results on Leaf Nitrogen Nutrient Content

The distribution of areas based on nitrogen content categories showed that most of the land fell into the slight deficiency (2.3–2.5%) and normal (2.5–2.7%) categories. OK and the UK mapped nearly equal areas for both categories (~990–1,038 thousand ha). The IDW tended to map a larger area as deficient (83,514 ha) and a slightly smaller area as normal. The RBF method mapped a higher deficiency (70,550 ha) compared to OK and UK, but was still lower than that of IDW. Areas with very high nitrogen content (>2.9%) appeared only in very small amounts (92 ha) and were not detected by OK. The complete area distribution data are presented in Table 4 and their spatial distributions are shown in Figure 3.

The distribution of phosphorus areas showed a striking difference among the methods, with the UK and RBF signifying a lower deficiency (~91–184 thousand hectares) compared to IDW (179 thousand hectares) and OK (149 thousand hectares). IDW and the UK classified more areas in the Slight Deficiency category (over 1,285,000 ha). RBF had the most proportional distribution, with the highest number in the normal category (750,685 ha) and a moderate proportion in the light deficiency and slightly excess categories. Only the OK and UK methods detected areas with excess phosphorus (>0.185%), although the amounts were very small (63 ha). The complete area distribution data are presented in Table 5 and their spatial distributions are shown in Figure 4. Most of the areas (>1,850,000 ha) fell into the normal category (0.80–1.00%) for all methods, with OK and the UK showing the highest values.

Table 3: T-Test Results of Actual and Predicted Values for Each Nutrient Content

Nutrient Content	Method	Actual Mean	Prediction Mean	T-Statistic
Nitrogen	IDW	0.155	0.155	0.337
	OK	0.155	0.155	-0.059
	UK	0.155	0.155	-0.125
	RBF	0.155	0.155	-0.037
Phosphorus	IDW	0.915	0.915	-0.034
	OK	0.915	0.915	-0.197
	UK	0.915	0.915	-0.046
	RBF	0.915	0.915	0.049
Potassium	IDW	0.915	0.915	-0.034
	OK	0.915	0.915	-0.197
	UK	0.915	0.915	-0.046
	RBF	0.915	0.915	0.049
Calcium	IDW	0.271	0.271	0.081
	OK	0.270	0.271	-0.553
	UK	0.270	0.271	-0.561
	RBF	0.270	0.271	-0.339
Magnesium	IDW	0.271	0.271	0.081
	OK	0.270	0.271	-0.553
	UK	0.270	0.271	-0.561
	RBF	0.270	0.271	-0.339

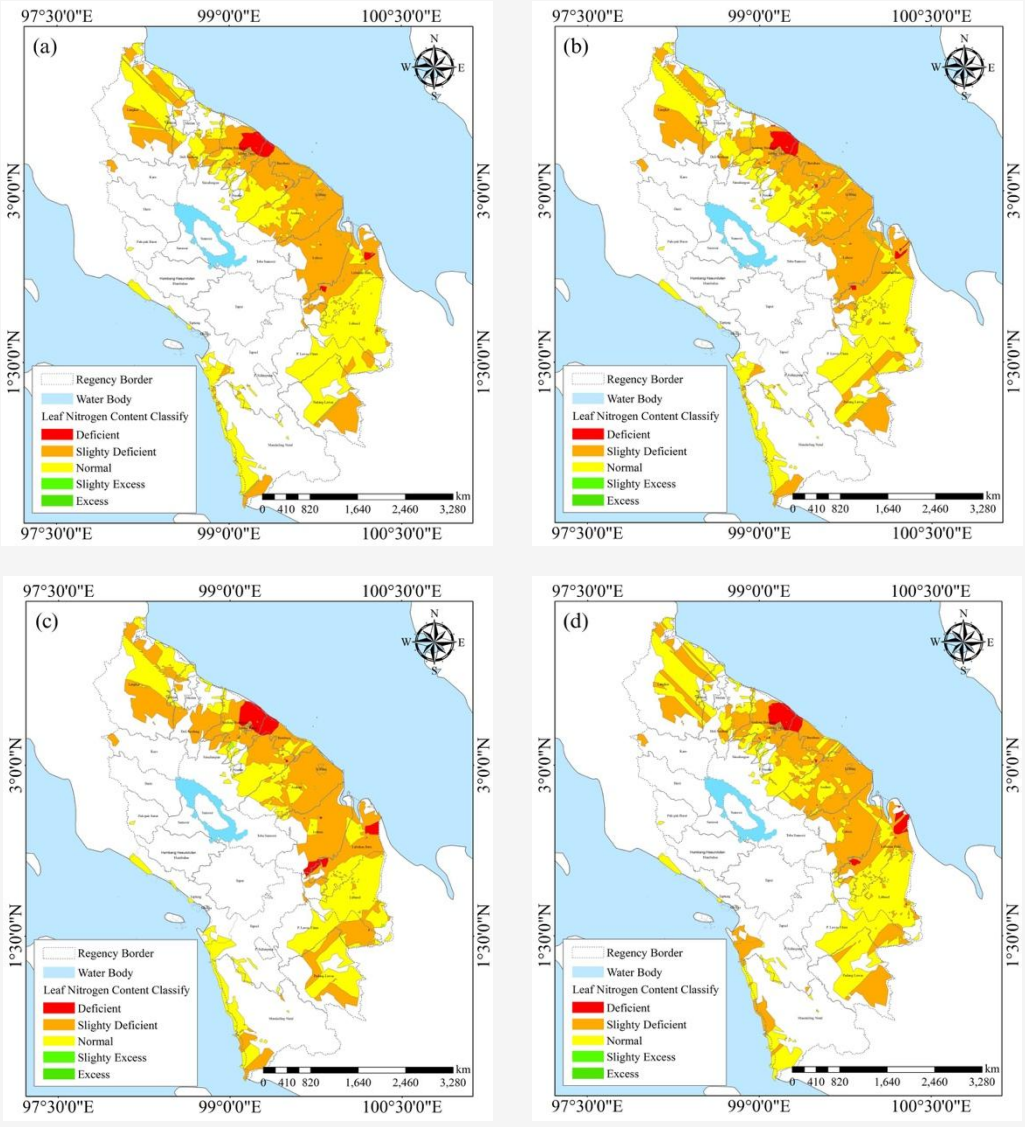

Figure 3: Spatial distribution of Nitrogen nutrient content in oil palm leaf: (a) ordinary kriging; (b) universal kriging; (c) radial basis function; and (d) inverse distance weighting

Table 4: Distribution of the area of nitrogen nutrient content from spatial analysis

Nitrogen Nutrient Content (%)		Area (hectares) OK	UK	IDW	RBF
Deficiency	<2.3	48,222	44,720	83,514	70,550
Slight Deficiency	2.3-2.5	990,617	1,025,429	1,036,997	974,786
Normal	2.5-2.7	1,038,622	1,006,682	955,001	1,030,557
Slightly Excess	2.7-2.9	1,566	2,105	3,423	3,042
Excess	>2.9	-	92	92	92
	Total	2,079,027	2,079,027	2,079,027	2,079,027

Description: Ordinary Kriging (OK); Universal Kriging (UK); Inverse Distance Weighting (IDW); RBF (Radial Basis Function)

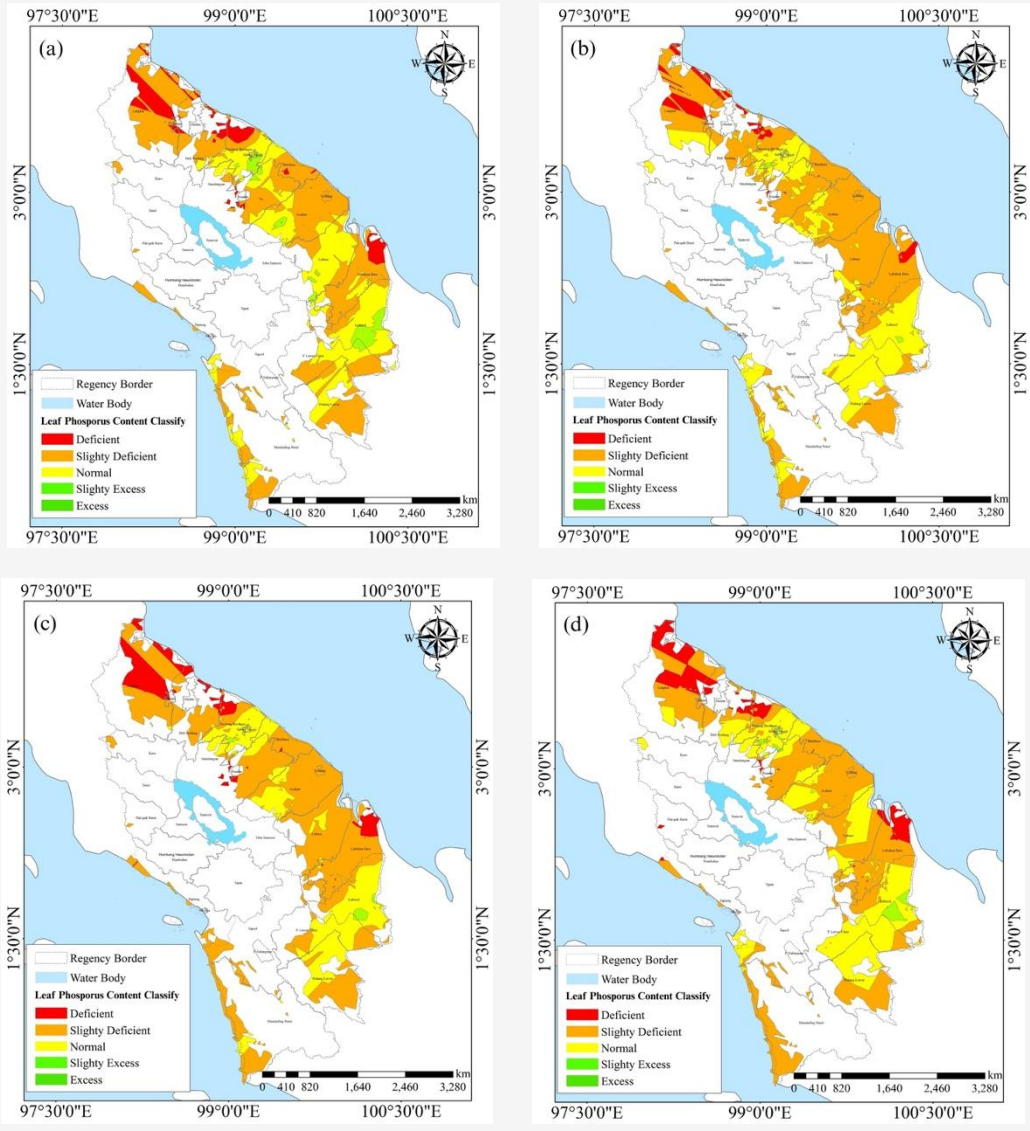

Figure 4: Spatial distribution of Phosphorus nutrient content of oil palm leaf: (a) ordinary kriging; (b) universal kriging; (c) radial basis function; and (d) inverse distance weighting

Table 5: Area distribution of phosphorus nutrient content from spatial analysis

Phosphorus Nutrient Content (%)		**Area (hectares)**			
		OK	**UK**	**OK**	**RBF**
Deficiency	<0.140	149,312	91,586	179,042	184,208
Slight Deficiency	0.140-0.155	1,138,582	1,285,176	1,334,193	1,110,498
Normal	0.155-0.170	712,148	694,245	549,526	750,685
Slightly Excess	0.170-0.185	78,922	7,957	16,266	33,573
Excess	>0.185	63	63	-	63
	Total	2,079,027	2,079,027	2,079,027	2,079,027

Description: Ordinary Kriging (OK); Universal Kriging (UK); Inverse Distance Weighting (IDW); RBF (Radial Basis Function)

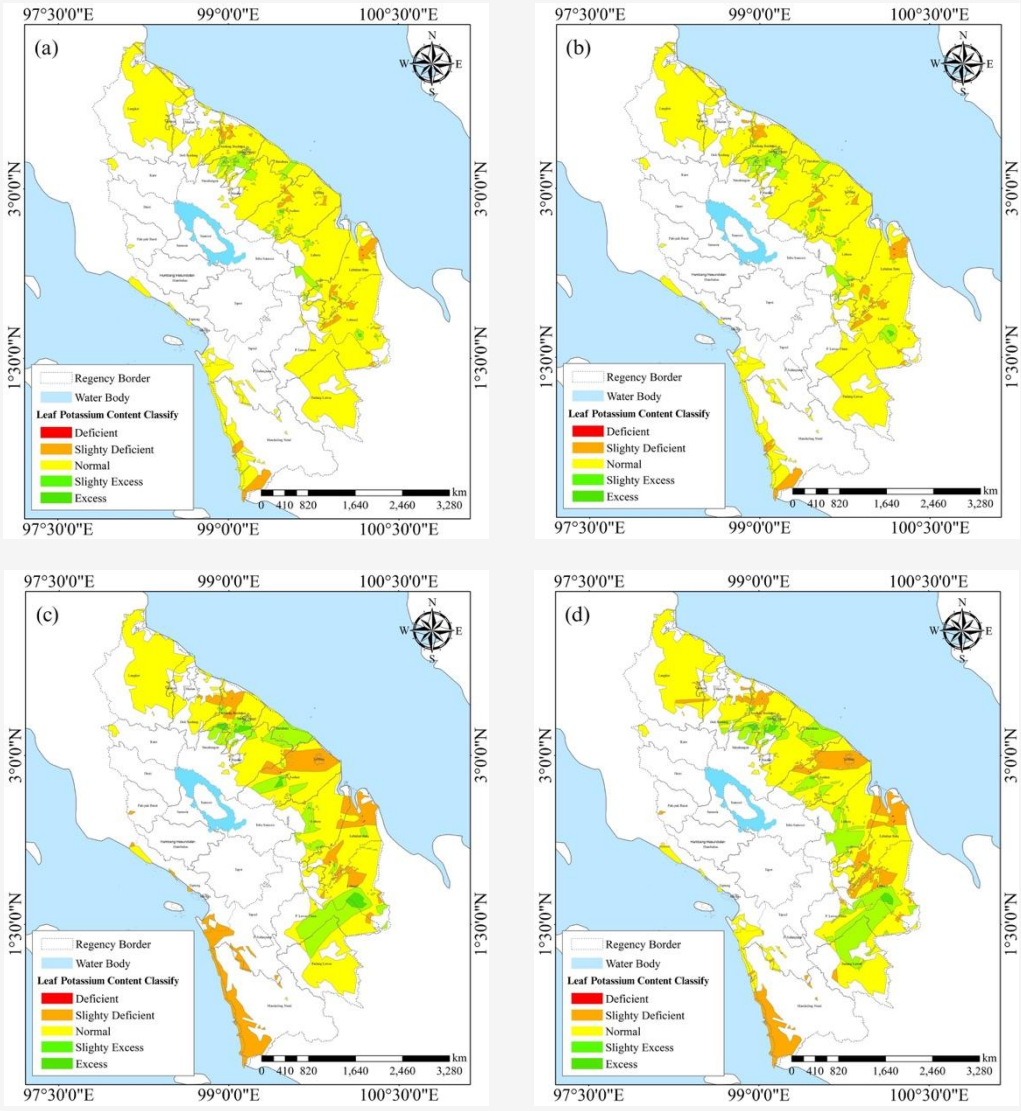

Figure 5: Spatial distribution of Potassium nutrient content of oil palm leaf: (a) ordinary kriging; (b) universal kriging; (c) radial basis function; and (d) inverse distance weighting

Table 6: Area distribution of potassium nutrient content from spatial analysis

Potassium Nutrient Content (%)		Area (hectares)			
		OK	UK	IDW	RBF
Deficiency	<0.60	337	188	492	617
Slight Deficiency	0.60-0.80	94,057	106,926	397,775	333,228
Normal	0.80-1.00	1,889,539	1,850,651	1,330,488	1,353,599
Slightly Excess	1.00-1.20	91,068	116,147	322,054	375,145
Excess	>1.20	4,026	5,116	28,218	16,439
	Total	2,079,027	2,079,027	2,079,027	2,079,027

Description: Ordinary Kriging (OK); Universal Kriging (UK); Inverse Distance Weighting (IDW); RBF (Radial Basis Function)

However, IDW and RBF tended to spread the predictions into light deficiency and slightly excess categories, suggesting that these two methods were more sensitive to variations around the threshold values. IDW mapped K deficiency at 492 ha, which was higher than that measured from OK (337 ha), and RBF produced a significantly higher result (617 ha). In the Excess category (>1.20%), IDW mapped the largest area (28,218 ha), representing broader extreme predictions. The complete data on area distribution are presented in Table 6, and the spatial distribution is shown in Figure 5.

The distribution of calcium content showed that OK and UK mapped excess areas (>0.70%) more broadly (~544 thousand hectares) than the other methods. RBF showed a much wider distribution of deficiencies (170,659 ha) than the other methods, followed by IDW (138,630 ha). The normal area (0.60–0.65%) tended to be lower in RBF (479,475 ha) than in OK (682,736 ha) and the UK (692,839 ha). This suggests that RBF and IDW were more aggressive in identifying values outside the normal range, while OK and UK were more conservative. The complete data on the area distribution obtained from the interpolation of the calcium nutrient content are presented in Table 7, and the spatial distribution is presented in Figure 6.

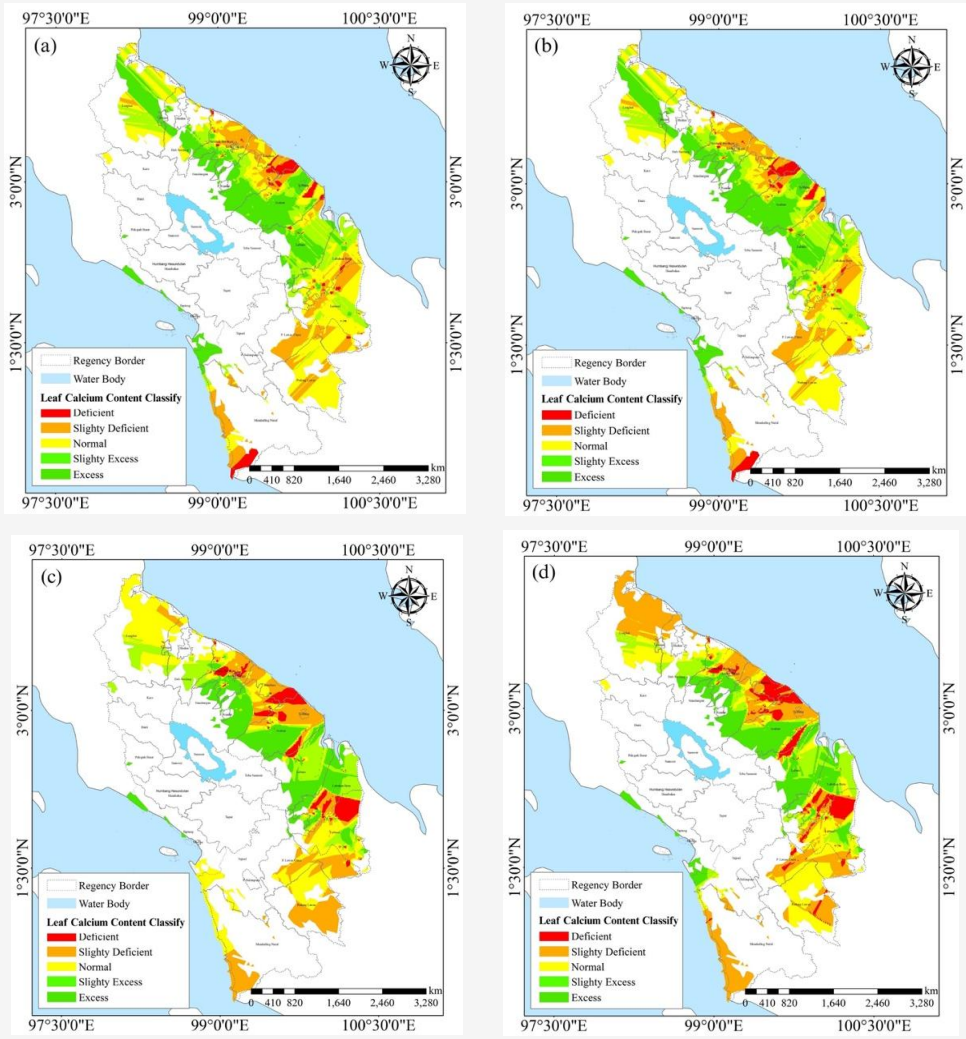

Figure 6: Spatial distribution of calcium nutrient content of oil palm leaf: (a) ordinary kriging; (b) universal kriging; (c) radial basis function; and (d) inverse distance weighting

Table 7: Area distribution of Calcium nutrient content from spatial analysis

Calcium Nutrient Content (%)		Area (hectares)			
		OK	UK	IDW	RBF
Deficiency	<0,55	71,430	72,161	138,630	170,659
Slight Deficiency	0,55-0,60	399,856	389,954	506,765	660,583
Normal	0,60-0,65	682,736	692,839	642,361	479,475
Slightly Excess	0,65-0,70	380,237	380,014	328,303	280,083
Excess	>0,70	544,767	544,059	462,967	488,226
	Total	2,079,027	2,079,027	2,079,027	2,079,027

Description: Ordinary Kriging (OK), Universal Kriging (UK), Inverse Distance Weighting (IDW), (Radial Basis Function);

Magnesium distribution showed that IDW and RBF mapped significantly more widespread deficiencies (>360 thousand hectares) compared to OK and UK (~263 thousand hectares). The RBF specifically mapped light deficiency and deficiency areas more extensively (total >775 thousand hectares), showing potential underestimation using this method. However, OK and the UK classified more land into Normal and Excess categories, reflecting more balanced and stable predictions. IDW had the highest normal area (639,749 ha), with a considerable distribution in the light deficiency and excess categories. The complete data on the area distribution resulting from the interpolation of the magnesium nutrient content are presented in Table 8, and the spatial distribution is presented in Figure 7.

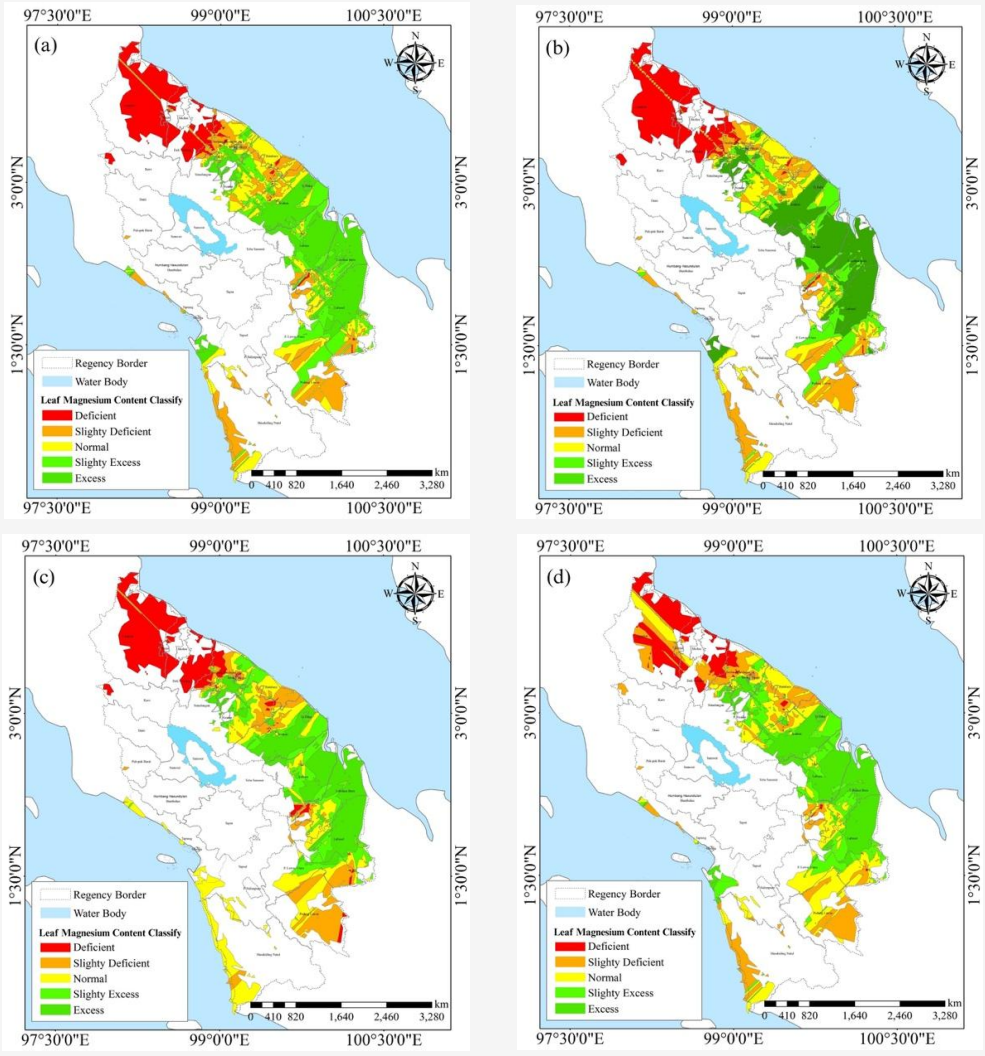

Figure 7: Spatial distribution of Magnesium nutrient content of oil palm leaf: (a) ordinary kriging; (b) universal kriging; (c) radial basis function; and (d) inverse distance weighting

Table 8: Area distribution of Magnesium nutrient content from spatial analysis

Magnesium Nutrient Content (%)		Area (hectares)			
		OK	UK	IDW	RBF
Deficiency	<0.20	263,320	263,020	360,640	384,149
Slight Deficiency	0.20-0.23	301,526	301,001	258,949	391,121
Normal	0.23-0.25	587,024	588,424	639,749	525,511
Slightly Excess	0.25-0.27	471,144	468,711	367,296	343,305
Excess	>0.27	456,012	457,871	452,394	434,941
	Total	2,079,027	2,079,027	2,079,027	2,079,027

Description: Ordinary Kriging (OK); Universal Kriging (UK); Inverse Distance Weighting (IDW); RBF (Radial Basis Function)

3.4 Spatial Model Accuracy Performance

The accuracy performance of the spatial models developed using the OK, UK, IDW, and RBF methods was evaluated using five statistical parameters: Mean Error (ME), Mean Absolute Error (MAE), Root Mean Square Error (RMSE), and accuracy (Acc). In the estimation of nitrogen content, all interpolation methods showed uniform ME values of 0.001, representing a very low level of bias. The MAE values were in a relatively narrow range, at 0.098 for IDW and between 0.112 and 0.114 for OK, the UK, and RBF, respectively. The lowest MSE and RMSE values were obtained using the IDW method, at 0.018 and 0.135, respectively. Meanwhile, the OK, UK, and RBF had MSE and RMSE values of 0.026 and 0.160, respectively. The accuracy of all methods in modelling nitrogen content was above 90%, with OK producing the highest accuracy value of 0.99.

Regarding phosphorus content, the ME, MAE, MSE, and RMSE calculations for the four interpolation methods produced values close to zero, ranging from 0.00–0.08. This suggests that all methods provided very good estimations of the spatial distribution of phosphorus. The accuracy levels achieved by the OK, UK, IDW, and RBF were high, ranging from 0.96–0.97. Similar results were obtained in the potassium content analysis, where the ME values for all four interpolation methods were close to zero, signifying no systematic bias in the predictions. The MAE, MSE, and RMSE values range from 0.101 to 0.104, 0.260 to 0.270, and 0.162 to 0.164, respectively. The prediction accuracy for potassium content ranged from 0.878 to 0.882, showing relatively consistent and high performance across all the methods.

The evaluation results for the calcium nutrient content showed very small ME values (0.000–0.001). The MAE ranged from 0.101 to 0.104, while the MSE and RMSE values were between 0.019–0.020 and 0.139–0.140, respectively. The prediction accuracy for calcium was above 80%, with values between 0.839 and 0.844, suggesting that the interpolation methods were capable of representing the spatial distribution of calcium, although slightly lower than that of nitrogen and phosphorus. The analysis of the magnesium content showed relatively variable results, which were still acceptable. The ME, MAE, MSE, and RMSE values were 0.001–0.003, 0.032–0.047, 0.020–0.040, and 0.045–0.065, respectively. The prediction accuracy obtained from OK, UK, IDW, and RBF for Mg ranged from 0.828 to 0.879. This suggests that all interpolation methods spatially modelled the magnesium content quite optimally, but there were slight differences in precision among the methods. In general, the evaluation results of the five leaf nutrients (N, P, K, Ca, and Mg) showed that the four interpolation methods were capable of providing good estimation results, as evidenced by the low error values (ME, MAE, MSE, and RMSE) and high accuracy levels.

IDW tended to produce the lowest error for nitrogen, whereas RBF and UK provided relatively stable performances for the other elements. The comparison graphs of the error values for each interpolation method and the individual nutrient elements measured are presented in Figure 8. The spatial structure of the leaf nutrient distribution was evaluated using empirical semivariogram modelling for each interpolation method and nutrient type. Table 9 presents the results of the fitted semivariogram parameters, including the selected model type, nugget, sill, nugget-to-sill ratio, spatial range, and the degree of spatial dependence. All interpolation methods (IDW, OK, UK, and RBF) and nutrients (Nitrogen, Phosphorus, Potassium, Calcium, and Magnesium) showed spatial patterns that were best described by the spherical model. This model has been widely recognized for its suitability in representing natural phenomena with continuous but bounded spatial correlations, particularly in soil and plant nutrient studies.

Table 9: Semivariogram parameters and spatial dependence

Nutrient	Method	Model	Nugget	Sill	Nugget/Sill Ratio (%)	Range (m)	Spatial Dependence
Nitrogen	OK	Spherical	0.000	0.021	0.000	462	Strong
	UK	Spherical	0.000	0.021	0.000	472	Strong
Phosphorus	OK	Spherical	0.000	7.860	0.000	3136	Strong
	UK	Spherical	0.000	4.800	0.000	3137	Strong
Potassium	OK	Spherical	0.000	0.025	0.000	455	Strong
	UK	Spherical	0.000	0.025	0.000	451	Strong
Calcium	OK	Spherical	0.000	0.018	0.000	357	Strong
	UK	Spherical	0.000	0.018	0.000	355	Strong
Magnesium	OK	Spherical	0.000	0.005	0.000	3136	Strong
	UK	Spherical	0.000	0.006	0.000	3136	Strong

Description: Ordinary Kriging (OK); Universal Kriging (UK)

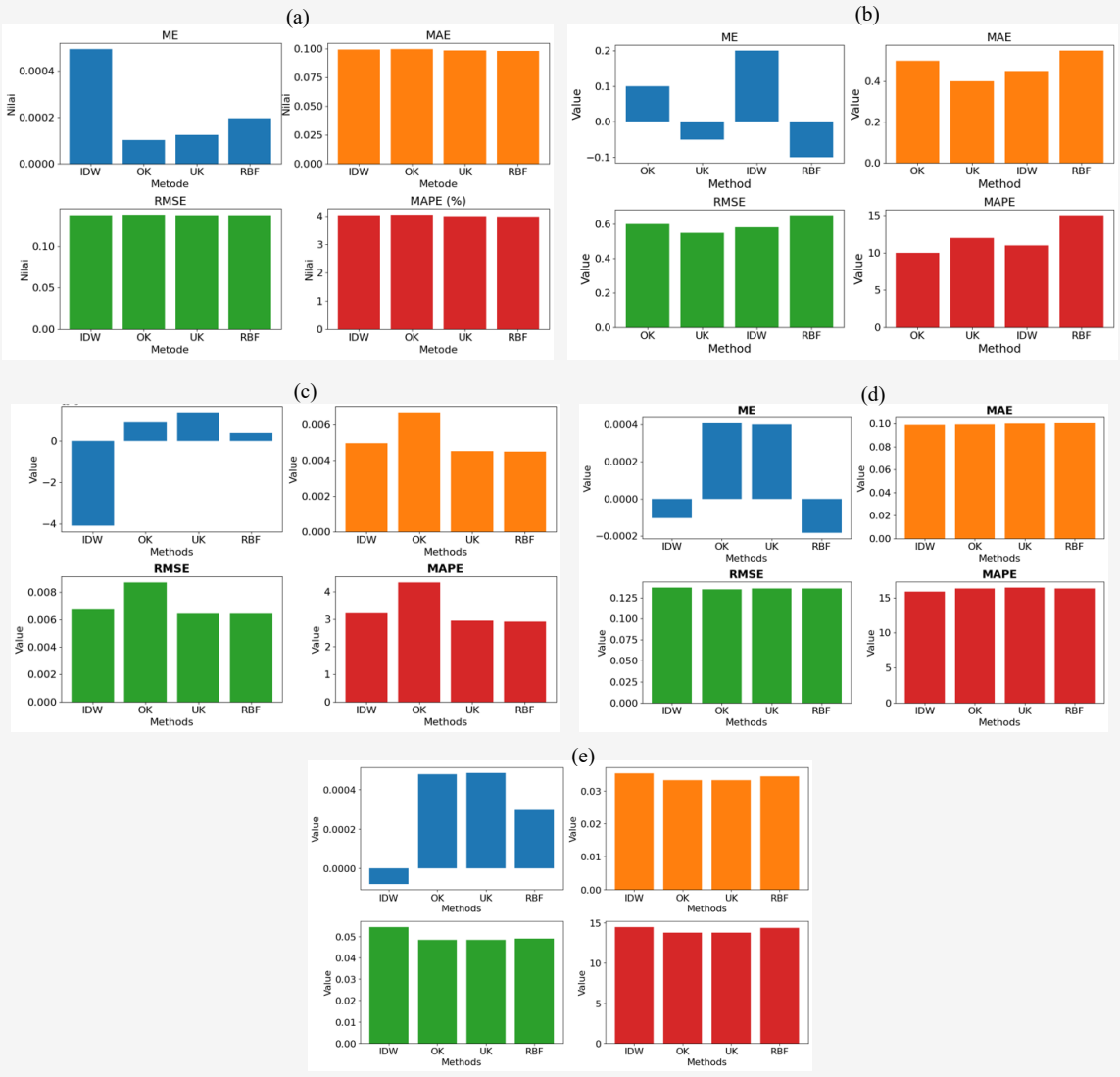

Figure 8: Bar chart values of ME, MAE, MSE, and RMSE in calculating the model estimation accuracy: (a) nitrogen, (b) phosphorus, (c) potassium, (d) calcium, and (e) magnesium

Across all nutrients and interpolation methods (OK and UK), the nugget effect was consistently zero, indicating negligible measurement errors and high precision in both data collection and semivariogram modeling. The sill values varied among nutrients, with Phosphorus exhibiting the highest sill values (4.80–7.86), followed by Potassium (0.025), Nitrogen (0.0214), Calcium (0.0186–0.0187), and Magnesium (0.0050–0.0058). These sill values represent the point at which the semivariogram levels off, signifying the total variance accounted for in the spatial structure. The nugget-to-sill ratio for all variables and methods was 0%, confirming strong spatial dependence according to established classification criteria (ratio < 25%) [25]. This suggests that the spatial variability of each nutrient is predominantly governed by structured spatial processes rather than random noise. The range values, which define the distance beyond which spatial autocorrelation becomes insignificant, also differed among nutrients. Nitrogen and Potassium exhibited moderate spatial ranges (451–472 m and 451–455 m, respectively), whereas Phosphorus and Magnesium displayed much broader spatial continuity (≈3136–3137 m), suggesting large-scale spatial correlation potentially linked to landscape-level or management factors. Calcium showed a shorter spatial range (≈355–357 m), indicating more localized spatial dependence. Collectively, these findings confirm that leaf nutrient data exhibit strong spatial autocorrelation under both OK and UK models, reinforcing the robustness and reliability of geostatistical interpolation approaches for precision agriculture applications.

Table 10: Prediction model of nutrient content of Nitrogen, Phosphorus, Potassium, Calcium, and Magnesium using interpolation in this study

Nutrient	Models	OK	UK	IDW	RBF
Nitrogen	Model	Y=0.474X+1.306	Y=0.489X+1.271	Y=0.471X+1.315	Y=0.490X+1.268
	R^2	0.509	0.514	0.513	0.0.514
Phosphorus	Model	Y=0.520X+0.074	Y=0.736X+0.041	Y=0.687X+0.049	Y=0.745X+0.040
	R^2	0.544	0.753	0.721	0.751
Potassium	Model	Y=0.526X+0.434	Y=0.522X+0.437	Y=0.487X+0.470	Y=0.558X+0.404
	R^2	0.541	0.540	0.525	0.544
Calcium	Model	Y=0.582X+0.295	Y=0.577X+0.299	Y=0.593X+0.287	Y=0.587X+0.291
	R^2	0.629	0.626	0.620	0.624
Magnesium	Model	Y=0.635X+0.099	Y=0.634X+0.099	Y=0.553X+0.121	Y=0.616X+0.104
	R^2	0.644	0.644	0.578	0.636

Description: Ordinary Kriging (OK); Universal Kriging (UK); Inverse Distance Weighting (IDW); RBF (Radial Basis Function)
X represents the actual nutrient values obtained from field measurements, while Y represents the predicted values generated by the interpolation models

3.5 Spatial Model of Nutrient Content

Based on the regression analysis between the laboratory-measured nutrient concentrations (actual values) and those predicted by the interpolation methods, the resulting regression equations and coefficients of determination (R^2) are summarized in Table 10. The strength of the models, as evidenced by the R^2 values, varied depending on the nutrient type and the interpolation method applied. For nitrogen, the coefficient of determination ranged from 0.509 to 0.514, indicating a moderate correlation between actual and predicted values, consistent with the classification in a previous study [26]. In the case of phosphorus, the models derived from OK, UK, and RBF showed strong predictive performance with identical R^2 values of 0.753, while the IDW method yielded a slightly lower R^2 of 0.721, which is considered moderate [26].

Predictions of potassium nutrient content demonstrated moderate correlations across all interpolation methods, with R^2 values ranging from 0.525 to 0.544. Similarly, the calcium models showed moderate predictive strength, with R^2 values between 0.620 and 0.629 across the four interpolation methods. The magnesium models also exhibited moderate predictive performance, with R^2 values spanning from 0.578 to 0.644. Scatterplots illustrating the distribution patterns of actual versus predicted values for each nutrient (N, P, K, Ca, and Mg) are presented in Figure 9. These visualizations support the statistical results and highlight the consistency of the spatial models in estimating nutrient concentrations across the different interpolation methods.

4. Discussion

This study aimed to map the distribution of oil palm leaf nutrient content using several geospatial analyses, including OK, the UK, IDW, and RBF. Four spatial analyses were applied to the macronutrient content of the oil palm: N, phosphorus, K, Ca, and Mg. This study found that geospatial analysis using OK, UK, IDW, and RBF obtained similar results in estimating the macronutrient content of nitrogen, phosphorus, K, and Mg in oil palm leaves.

The results of the descriptive analysis showed that the ranges of the minimum, maximum, average, standard deviation (SD), and CV values of the four spatial interpolation methods were relatively the same. The minimum, maximum, mean, SD, and CV range of values included 1.92–1.955%, 2.82–2.97%, 2.48–2.49%, 0.02, and 5.12–5.47% for nitrogen, 0.12–0.13%, 0.18–0.19%, 0.16%, 0.01, and 5.83–7.31% for phosphorus, 0.54–0.63%, 1.54–1.65%, 0.90–0.91%, 0.02–0.15, and 0.78–17.31% for potassium, 0.18–0.33%, 1.21–1.33%, 0.72%, 0.14, and 24.13–24.62% for calcium, as well as 0.08–0.10%, 0.46–0.52%, 0.27%, 0.04–0.05, and 19.05–24.16% for magnesium, respectively. Based on previous studies [23], CV values for geospatial analysis using OK, UK, IDW, and RBF to evaluate the nutrient contents in oil palm leaves showed low variability for nitrogen, phosphorus, potassium, and magnesium, while calcium had moderate variability.According to the coefficient of determination (R^2), the predictions for nitrogen, phosphorus, potassium, calcium, and magnesium ranged [from 0.51 to 0.56, 0.73 to 0.76, 0.49 to 0.54, 0.65 to 0.67, and 0.51 to 0.62, respectively.

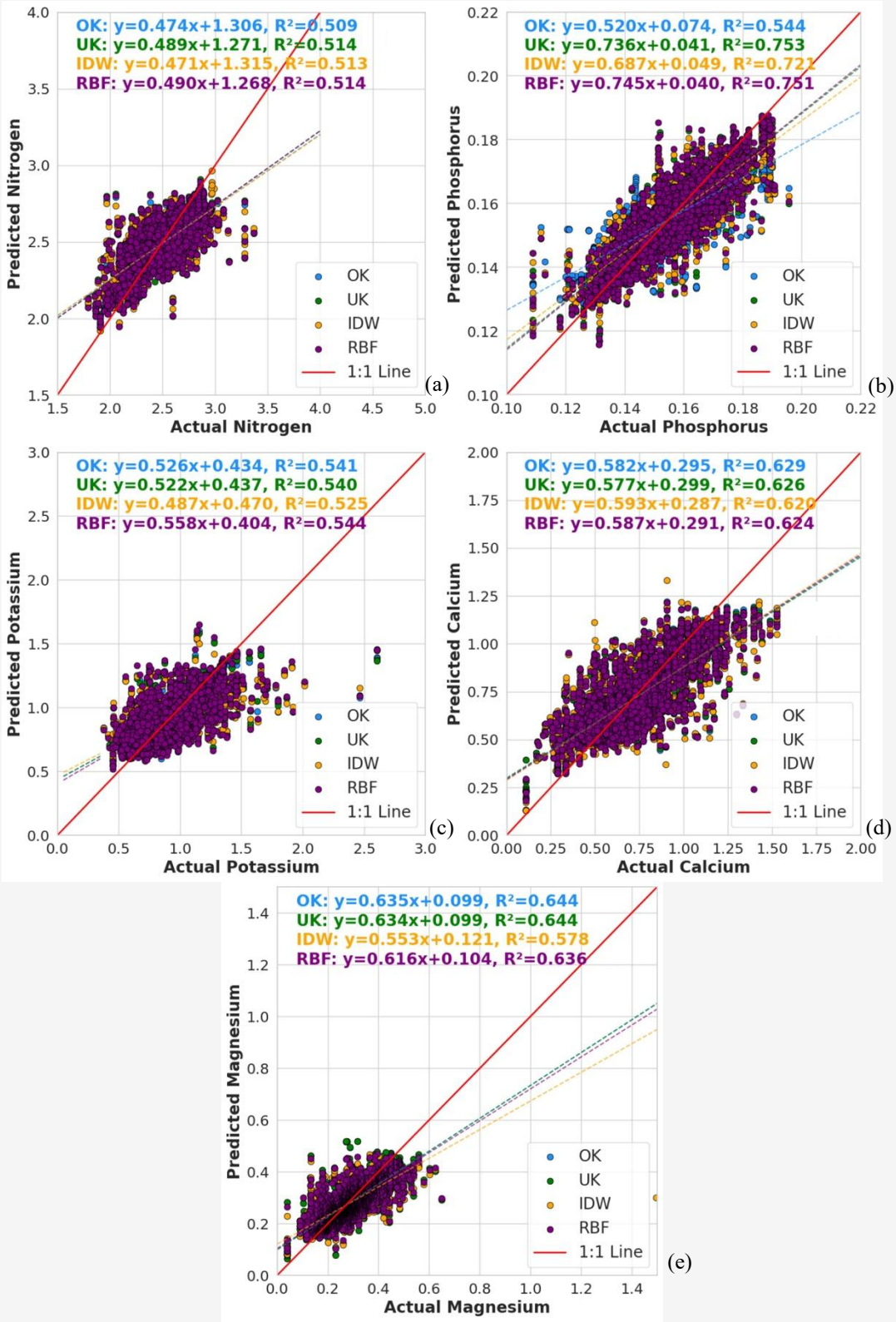

Figure 9: Relationship between actual and estimated leaf nutrient conten using OK, UK, IDW, and RBF for: (a) nitrogen, (b) phosphorus, (c) potassium, (d) calcium, and (e) magnesium

These values represented strong correlations between the observed and predicted nutrient levels, as supported by previous studies [27] and [28]. The results showed that the OK, UK, IDW, and RBF methods produced highly reliable predictions of nutrient content.

The prediction performance evaluated using accuracy metrics such as ME, MAE, MSE, RMSE, and accuracy, produced consistent results across all interpolation methods. As shown in Figure 8, the average accuracy ranged between 0.96 and 0.97, reflecting excellent predictive capability. Consequently, all four geospatial interpolation methods OK, UK, IDW, and RBF produced reliable estimates for the 3,191 oil palm leaf samples analyzed. These results correspond with those of previous studies, which also emphasized the superiority of IDW and OK in producing estimates closest to the actual values [20][29][30][31][32][33] and [34]. Based on the paired t-test results comparing the actual and predicted mean nutrient contents across four interpolation methods (IDW, OK, UK, RBF), no statistically significant differences were found for any nutrient (Nitrogen, Phosphorus, K, Ca, or Mg). All p-values were greater than 0.05, indicating that the predicted values closely approximated actual laboratory measurements. This suggests that all four interpolation methods provided reliable estimations of leaf nutrient content with comparable accuracy in spatial prediction performance.

The semivariogram analysis conducted for each nutrient and interpolation method revealed consistently low nugget values (0.0000) across all the variables and methods. The sill values varied by nutrient type, but the resulting nugget-to-sill ratio was 0% in all cases, indicating a strong spatial dependence according to the established classification criteria [25]. The strong spatial structure observed across nitrogen, phosphorus, K, Ca, and Mg contents suggests that spatial variability in leaf nutrient concentrations is predominantly controlled by structured spatial patterns rather than random or measurement-related noise. This implies that these nutrients exhibited spatial autocorrelation at the examined scale, making them suitable for interpolation using geostatistical techniques.

Furthermore, the relatively long-range values observed for each nutrient (e.g., 3136 m for phosphorus and magnesium) indicate that spatial correlation extends over considerable distances. This is particularly advantageous for mapping and predicting nutrient distributions in oil palm plantations, because it suggests that sparse but well-distributed sampling can yield reliable spatial models. These results are consistent with recent findings, which emphasized that strong spatial dependence, as shown by nugget/sill ratios below 25%, enhances the precision of spatial interpolation in nutrient mapping. Thus, the use of the ordinary kriging (OK), universal kriging (UK), inverse distance weighting (IDW), and radial basis function (RBF) methods is justifiable and effective under strong spatial dependence conditions [35].

In a general context, no single interpolation method universally outperforms the others; however, each has distinct advantages. OK is effective for stable and balanced predictions, UK shows suitability for capturing broader spatial trends, IDW is ideal for detecting local nutrient anomalies, and RBF offers smoother surface predictions. Therefore, interpolation methods should be selected based on data characteristics and management objectives, particularly for site-specific nutrient management in oil palm plantations.

5. Conclusion

This study highlights the effectiveness of four spatial interpolation methods, Ordinary Kriging (OK), Universal Kriging (UK), Inverse Distance Weighting (IDW), and Radial Basis Function (RBF), to accurately estimate the spatial distribution of key macronutrients (N, P, K, Ca, and Mg) in oil palm leaves. Descriptive statistical analysis revealed that nitrogen, phosphorus, and Mg exhibited low spatial variability and consistent central tendency measures across all methods, indicating their uniform distribution and stability in the plantation environment. In contrast, K and Ca displayed higher spatial heterogeneity, with elevated coefficients of variation and skewed distributions, suggesting the influence of site-specific soil and management factors.

The t-test analysis showed no significant differences between the actual and predicted values for all nutrients and methods, thereby confirming the statistical reliability of the interpolation models. Spatial distribution maps further demonstrated that OK and UK produced more conservative and balanced predictions, whereas IDW and RBF were more responsive to local variations and extremes. The model accuracy evaluation supported these findings, with all methods achieving high accuracy scores (≥0.83), particularly for nitrogen and phosphorus. Semivariogram modeling revealed a strong spatial dependence (nugget-to-sill ratio = 0%) and significant spatial ranges, particularly for phosphorus and magnesium (>3 km), validating the suitability of geostatistical approaches for nutrient mapping. Regression analyses yielded moderate to strong correlations (R^2 = 0.51–0.76), particularly for

phosphorus, reinforcing the predictive strength of the spatial models.

In conclusion, all four interpolation methods yielded reliable nutrient predictions, each offering distinct advantages based on the nutrient type and spatial variability. These findings highlight the importance of selecting suitable interpolation techniques based on the nutrient characteristics and management objectives. These spatial models are robust tools for precision agriculture, facilitating site-specific nutrient management to boost oil palm productivity and resource efficiency. To advance future research, it is advisable to integrate remote sensing data with machine-learning techniques to enhance prediction accuracy. Furthermore, broadening the spatial coverage of sampling and incorporating temporal monitoring would offer a more comprehensive representation of the seasonal variability in nutrient dynamics. These approaches are anticipated to strengthen the robustness and applicability of geospatial analyses in nutrient mapping of oil palm plantations.

Acknowledgement
The authors are grateful to the Indonesian Oil Palm Research Institute (IOPRI) for funding this study.

Reference

[1] Corley, R. H.V. and Tinker, P. B., (2016). *The Oil Palm*. Fifth Edition. John Wiley and Sons, Ltd., Chichester, West Sussex, UK.

[2] Goh, K. J. and Hardter, R., (2003). General Oil Palm Nutrition. In Fairhurst, T. and Hardter, R. (Eds.), *Oil Palm Management for Large and Sustainable Yields*. International Plant Nutrition Institute, Penang, Malaysia. 191–230

[3] Ginting, E. N. and Sutarta, E. S., (2013). Peningkatan Efisiensi Pemupukan Melalui Pendekatan Konsep Keseimbangan Hara dalam Upaya Menuju Perkebunan Sawit Lestari [Improving Fertilization Efficiency Using Nutrient Balance Approach Toward Sustainable Oil Palm Plantation]. In Yeni, Y. et al. (Eds.), *Pertemuan Teknis Kelapa Sawit 2013 – Strategi Menuju Produktivitas Tinggi dan Lestari*. Pusat Penelitian Kelapa Sawit, Bali. 55–65.

[4] Darmawan, S., Hernawati, R., Hariandi, F., Wiratmoko, D., and Permadi, D. (2024). Development of Spatial Database System Based on Cloud Computing Remote Sensing for Monitoring of Oil Palm Plantation in Indonesia. *International Journal of Geoinformatics*, Vol. 20(11), 39–53. https://doi.org/10.52939/ijg.v20i11.3683.

[5] Comte, I., Colin, F., Grünberger, O., Follain, S., Whalen, J. K. and Caliman, J. P., (2013). Landscape-Scale Assessment of Soil Response to Long-Term Organic and Mineral Fertilizer Application in an Industrial Oil Palm Plantation in Indonesia. *Agriculture, Ecosystems and Environment*, Vol. 169, 58–68. https://doi.org/10.1016/j.agee.2013.02.010.

[6] Mat Su, A. S. and Tan, S. Q., (2019). A Review of Fertilization Assessment Methods for Oil Palm Plantations. *Konvensyen Kebangsaan Kejuruteraan Pertanian dan Makanan 2019*. Ministry of Agriculture and Agro-Based Industry Malaysia, Putrajaya.

[7] Pasuquin, J. M., Cock, J., Donough, C. R., Oberthur, T., Rahmadsyah, Lubis, A., Abdurrohim, G., Indrasuara, K., Dolong, T. and Cook, S., (2014). Leaf Nutrient Analysis as a Management Tool in Yield Intensification of Oil Palm. *Better Crops*, Vol. 98(1), 18–21.

[8] Fairhurst, T. and Hardter, R., (2003). *Oil Palm: Management for Large and Sustainable Yields* (Eds.). International Plant Nutrition Institute, Penang, Malaysia. 231–257.

[9] Khan, M. Z., Islam, M. R., Salam, A. B. A. and Ray, T., (2021). Spatial Variability and Geostatistical Analysis of Soil Properties in the Diversified Cropping Regions of Bangladesh Using Geographic Information System Techniques. *Applied and Environmental Soil Science*, Vol. 2021, 1–15. https://doi.org/10.1155/2021/6639180.

[10] Shen, Q., Wang, Y., Wang, X., Liu, X., Zhang, X. and Zhang, S., (2019). Comparing Interpolation Methods to Predict Soil Total Phosphorus in the Mollisol Area of Northeast China. *Catena*, Vol. 174, 59–72. https://doi.org/10.1016/j.catena.2018.10.052.

[11] Dong, W., Wu, T., Luo, J., Sun, Y. and Xia, L., (2019). Land Parcel-Based Digital Soil Mapping of Soil Nutrient Properties in an Alluvial-Diluvia Plain Agricultural Area in China. *Geoderma*, Vol. 340, 234–248. https://doi.org/10.1016/j.geoderma.2019.01.018.

[12] Gao, L., Huang, M., Zhang, W., Qiao, L., Wang, G. and Zhang, X., (2021). Comparative Study on Spatial Digital Mapping Methods of Soil Nutrients Based on Different Geospatial Technologies. *Sustainability*, Vol. 13(6). https://doi.org/10.3390/su13063270.

[13] Mueller, T. G., Pusuluri, N. B., Mathias, K. K., Cornelius, P. L., Barnhisel, R. I. and Shearer, S. A., (1996). Map Quality for Ordinary Kriging and Inverse Distance Weighted Interpolation. *Soil Science Society of America Journal*, Vol. 70, 1021–1029.

[14] Tiruneh, G. A., Alemayehu, T. Y., Meshesha, D. T., Adgo, E. and Reichert, J. M., (2023). Variability Modeling and Mapping of Soil Properties for Improved Management in Ethiopia. *Agrosystems, Geosciences and Environment*, Vol. 6(1), 1–12. https://doi.org/10.1002/agg2.20357.

[15] Kim, E., Nam, S.H., Ahn, C.H., Lee, S., Koo, J. W. and Hwang, T. M., (2022). Comparison of Spatial Interpolation Methods for Distribution Map Using Unmanned Surface Vehicle Data for Chlorophyll-A Monitoring in the Stream. *Environmental Technology and Innovation*, Vol. 28. https://doi.org/10.1016/j.eti.2022.102637

[16] Ismail, S., Ya'acob, N., Kassim, M., and Nik Dzulkefli, N. (2025). Seasonal Monitoring and Analysis of Soil Moisture and Vegetation Health in Oil Palm Plantations Using Remote Sensing. *International Journal of Geoinformatics*, Vol. 21(4), 82–96. https://doi.org/10.52939/ijg.v21i4.4069.

[17] Uexkull, H. R. von and Fairhurst, T. H., (1992). *Fertilizing for High Yield and Quality: Oil Palm*. IPI Bulletin No. 12. International Potash Institute, Singapore.

[18] Thammaboribal, P., Tripathi, N., and Lipiloet, S. (2024). Pre-Seismic Signature Detection using Diurnal GPS-TEC and Kriging Interpolation Maps (ASK-VTEC Technique): 11 May 2011, M9.0 Tohoku Earthquake Case Study. *International Journal of Geoinformatics*, Vol. 20(11), 148–161. https://doi.org/10.52939/ijg.v20i11.3715.

[19] Meng, Q., Liu, Z. and Borders, B. E., (2013). Assessment of Regression Kriging for Spatial Interpolation – Comparisons of Seven GIS Interpolation Methods. *Cartography and Geographic Information Science*, Vol. 40(1), 28–39. https://doi.org/10.1080/15230406.2013.762138.

[20] Liu, L., Jin, Y., Wang, J., Hong, Q., Pan, Z. and Zhao, J., (2019). Comparison of Spatial Interpolation Methods on Slowly Available Potassium in Soils. *IOP Conference Series: Earth and Environmental Science*, Vol. 234(1). https://doi.org/10.1088/1755-1315/234/1/012018.

[21] Meng, Q., Smith, S. A. and Rodgers, J., (2024). Geospatial Analysis and Mapping of Regional Landslide Susceptibility: A Case Study of Eastern Tennessee, USA. *GeoHazards*, Vol. 5(2), 364–373. https://doi.org/10.3390/geohazards5020019.

[22] Razi, N. M., Zakaria, S. N. S., Shahidin, N. M. and Nasron, N., (2022). Assessments of Nutrients Content in Soil and Leaves of Harumanis Mangoes and Its Relationship with the Yield. *IOP Conference Series: Earth and Environmental Science*, Vol. 1051(1). https://doi.org/10.1088/1755-1315/1051/1/012017.

[23] Kim, H. Y., (2013). Statistical Notes for Clinical Researchers: Assessing Normal Distribution (2) Using Skewness and Kurtosis. *Restorative Dentistry and Endodontics*, Vol. 38(1), 52–54. https://doi.org/10.5395/rde.2013.38.1.52.

[24] Fageria, V. D., (2001). Nutrient Interactions in Crop Plants. *Journal of Plant Nutrition*, Vol. 24, 1269–1290. https://doi.org/10.1081/PLN-100106981.

[25] Cambardella, C. A., Moorman, T. B., Novak, J. M., Parkin, T. B., Karlen, D. L., Turco, R. F. and Konopka, A. E., (1994). Field-Scale Variability of Soil Properties in Central Iowa Soils. *Soil Science Society of America Journal*, Vol. 58(5), 1501–1511. https://doi.org/10.2136/sssaj1994.03615995005800050033x.

[26] Hair, J. F., Black, W. C., Babin, B. J. and Anderson, R. E., (2019). *Multivariate Data Analysis* (8th Ed.). Cengage Learning.

[27] Sugiyono. (2006). *Statistika untuk Penelitian [Statistics for Research]* (6th Ed.). Alfabeta, Bandung.

[28] Man, A., Chaichana, C., Wicharuck, S. and Rinchumphu, D., (2022). Predicting Sunlight Availability for Vertical Shelves Using Simulation. *IOP Conference Series: Earth and Environmental Science*, Vol. 1094(1). https://doi.org/10.1088/1755-1315/1094/1/012011.

[29] Keshavarzi, A., Tuffour, H. O., Brevik, E. C. and Ertunç, G., (2021). Spatial Variability of Soil Mineral Fractions and Bulk Density in Northern Ireland: Assessing the Influence of Topography Using Different Interpolation Methods and Fractal Analysis. *Catena*, Vol. 207. https://doi.org/10.1016/j.catena.2021.105646.

[30] Huynh, C. V., Pham, T. G., Nguyen, L. H. K., Nguyen, H. T., Nguyen, P. T., Le, Q. N. P., Tran, P. T., Nguyen, M. T. H. and Tran, T. T. A., (2022). Application of GIS and Remote Sensing for Soil Organic Carbon Mapping in a Farm-Scale in the Hilly Area of Central Vietnam. *Air, Soil and Water Research*, Vol. 15, 1–13. https://doi.org/10.1177/11786221221114777.

[31] Wang, R., Zou, R., Liu, J., Liu, L. and Hu, Y., (2021). Spatial Distribution of Soil Nutrients in Farmland in a Hilly Region of the Pearl River Delta in China Based on Geostatistics and the Inverse Distance Weighting Method. *Agriculture*, Vol. 11(1), 1–12. https://doi.org/10.3390/agriculture11010050.

[32] Setianto, A. and Triandini, T., (2013). Comparison of Kriging and Inverse Distance Weighted (IDW) Interpolation Methods in Lineament Extraction and Analysis. *Journal of Southeast Asian Applied Geology*, Vol. 5(1), 21–29.

[33] Bhunia, G. S., Shit, P. K. and Maiti, R., (2018). Comparison of GIS-Based Interpolation Methods for Spatial Distribution of Soil Organic Carbon (SOC). *Journal of the Saudi Society of Agricultural Sciences*, Vol. 17(2), 114–126. https://doi.org/10.1016/j.jssas.2016.02.001.

[34] Wu, Y. H. and Hung, M. C., (2016). *Comparison of Spatial Interpolation Techniques Using Visualization and Quantitative Assessment.* Applications of Spatial Statistics. InTech. https://doi.org/10.5772/65996.

[35] Sun, G., Liu, H., Cui, D. and Chai, C., (2022). Spatial Heterogeneity of Soil Nutrients in Yili River Valley. *PeerJ*, Vol. 10. https://doi.org/10.7717/peerj.13311.